JOURNAL OF ENVIRONMENTAL SCIENCES XX (XXXX) XXX–XXX

Available online at www.sciencedirect.com

ScienceDirect

www.elsevier.com/locate/jes

JES JOURNAL OF ENVIRONMENTAL SCIENCES

www.jesc.ac.cn

Q1

Assessing the inter-annual variability of separation distances around odour sources to protect the residents from odour annoyance

Q3 Q2 *Marlon Brancher*[1,2,*], *Martin Piringer*[3], *Davide Franco*[1], *Paulo Belli Filho*[1], *Henrique De Melo Lisboa*[1], *Günther Schauberger*[2]

1. *Postgraduate Program in Environmental Engineering (PPGEA), Federal University of Santa Catarina (UFSC), 88040900, Florianópolis, Brazil. CAPES Foundation scholarship holder (main author), Brazilian Ministry of Education, Brasília, Brazil*

2. *WG Environmental Health, Department of Biomedical Sciences, University of Veterinary Medicine Vienna, Veterinärplatz 1, A-1210 Vienna, Austria*

3. *Central Institute for Meteorology and Geodynamics, Hohe Warte 38, A-1190 Vienna, Austria*

ARTICLE INFO

Article history:
Received 23 November 2017
Revised 15 September 2018
Accepted 18 September 2018
Available online xxxx

Keywords:
Environmental odour
Odour annoyance
Impact assessment
Dispersion modelling
Regulatory criteria
Separation distance

ABSTRACT

In recent years, there has been a growing concern about potential impacts on public health and wellbeing due to exposure to environmental odour. Separation distances between odour-emitting sources and residential areas can be calculated using dispersion models, as a means of protecting the neighbourhood from odour annoyance. This study investigates the suitability of using one single year of meteorological input data to calculate reliable direction-dependent separation distances. Accordingly, we assessed and quantified the inter-annual variability of separation distances at two sites with different meteorological conditions, one in Brazil and the other in Austria. A 5-year dataset of hourly meteorological observations was used for each site. Two odour impact criteria set in current regulations were selected to explore their effect on the separation distances. The coefficient of variation was used as a statistical measure to characterise the amount of annual variation. Overall, for all scenarios, the separation distances had a low degree of inter-annual variability (mean coefficient of variation values from 8% to 21%). Reasonable agreements from year to year were therefore observed at the two sites under investigation, showing that one year of meteorological data is a good compromise to achieve reliable accuracy. This finding can provide a more cost-effective solution to calculate separation distances in the vicinity of odour sources.

1. Introduction

Odour emissions have become a topic of increasing interest in both developed and developing countries worldwide. For many years now, environmental odour is the leading cause of public complaints reported to authorities regarding air quality (Hayes et al., 2014; Henshaw et al., 2006). Indeed, environmental odour is an ambient stressor since it is

* Corresponding author at: WG Environmental Health, Department of Biomedical Sciences, University of Veterinary Medicine Vienna, Veterinärplatz 1, A-1210 Vienna, Austria. Q4
E-mail address: marlon.b@posgrad.ufsc.br. (M. Brancher).

https://doi.org/10.1016/j.jes.2018.09.018
1001-0742

physically perceptible, negatively valued, unpredictable, uncontrollable and entails moderate adjustments (Campbell, 1983). In many jurisdictions, environmental odour is already handled as an air pollutant subject to specific legislation (Brancher et al., 2017). In the policy context of the European Union (EU), it is worth mention that, for the first time, odour has been considered in the Joint Research Centre Reference Report on monitoring of emissions to air and water from installations covered by the Industrial Emissions Directive 2010/75/EU (Brinkmann et al., 2018).

Odour exposure has been associated with health issues, affecting both the physiological and psychosocial status (Sucker et al., 2009). Physiological health symptoms comprise, for instance, headache, nausea, respiratory complications, tiredness, eye irritation and palpitations (Schiffman and Williams, 2005). Because dilution occurs in the atmosphere, odours often reach the population at concentrations far below toxicity thresholds, making direct toxicological mechanisms unlikely to explain the association between exposures and symptoms (Blanes-Vidal et al., 2014). Interestingly, epidemiological studies have shown indirect mechanisms in which psychosocial responses (i.e., odour annoyance) mediate physical symptom reporting (Blanes-Vidal, 2015). Hence, odour annoyance has been identified as one of the most important effects due to exposure to malodour (Cantuaria et al., 2017; Shusterman, 1992).

A suitable parameter to describe the influence of an odour source on the nearby residential area is the separation distance intended to embrace the area within which odour has the potential to cause annoyance (Piringer et al., 2015; Schauberger et al., 2000). The separation distance approach is part of an integrated multi-tool strategy recommended by Brancher et al. (2017) to manage environmental odours. The separation distance divides the area around odour-emitting facilities into two zones: (i) a zone beyond the separation distance where odour annoyance is likely to be avoided and (ii) a zone closer than the separation distance where loss of public amenity can be expected (Piringer et al., 2016). The separation distance can be fixed, given by pre-established distances; or variable, determined as direction-dependent distances on a case-by-case basis typically using dispersion models. In this case, time series of ambient odour concentration predicted by dispersion models are evaluated by so-called odour impact criteria OIC. As a result, separation distances between an odour source and residential areas are calculated, in a direction-dependent manner. Thereby, direction-dependent separation distances are the ultimate measure accounting for the entire chain from the odour emission rate, the dilution in the atmosphere, and the evaluation of the time series of ambient odour concentration by the OIC (Sommer-Quabach et al., 2014).

Nowadays, a wide range of OIC is in force, which shows that the assessment of odour annoyance varies greatly (Brancher et al., 2017; Griffiths, 2014; Sommer-Quabach et al., 2014). The OIC can be specified by three components: (i) the odour concentration threshold C_t (given in European odour units per cubic meter ou_E/m^3 or equivalent units), (ii) the percentile rank value P (also specified as exceedance probability 100 − P), and (iii) the averaging time A_t. Typically, dispersion models predict hourly time series of ambient odour concentrations (De Melo Lisboa et al., 2006; Drew et al., 2007). If the OIC are specified for an A_t shorter than 1 h, then a coefficient called peak-to-mean factor F comes into play. The F is used to estimate concentrations for shorter averaging times than that equivalent to the model output, as an attempt to mimic the odour perception of the human nose (Schauberger et al., 2012). A pioneering concept structured in the computation of ambient odour concentration variances to determine this F has been recently presented (Ferrero et al., 2017; Oettl and Ferrero, 2017; Oettl et al., 2018).

It is well known that, together with emissions, meteorological data play a central role in dispersion modelling (Capelli et al., 2013). Unsurprisingly, a critical methodological step in the calculation of separation distances using dispersion models is the acquisition, pre-processing and validation of meteorological data. In this regard, a key challenge is to calculate representative distances, while the meteorological input data is reduced. In addition, international regulatory requirements for odour dispersion modelling differ considerably in the sense that odour studies can be conducted on a monthly, annual or multi-year basis over the meteorological input data (Brancher et al., 2017). The year-to-year variation of odour contour lines, in particular, has been briefly touched by few technical reports (ERM, 2012; Featherston et al., 2014; GHD, 2015). However, the inter-annual variability of direction-dependent separation distances to avoid odour annoyance has yet to be explored. This knowledge is of relevance not only for future research but also for improving current odour regulations.

In this work, we investigated whether one single year of meteorological input data is enough to calculate reliable separation distances. For this purpose, we assessed and quantified the inter-annual variability of separation distances at two sites with different meteorological conditions. The calculations were undertaken for São José dos Pinhais (Brazil, near Curitiba) and Groß-Enzersdorf (Austria, near Vienna). Five years of hourly meteorological observations were used for each site. Modelling scenarios consider a point source with constant odour emission rate (annual mean value). Two national OIC were selected as references to calculate the separation distances.

2. Material and methods

2.1. Description of sites

The investigation was carried out at two sites, one in Brazil and the other in Austria, where yearly datasets of meteorological observations are available. Furthermore, we chose these sites because they meet the terrain requirements for performing modelling studies using a Gaussian plume model, and are representative of the odour sources found in the surrounding areas. São José dos Pinhais (−25.555° S, −49.132° W, 906 m ASL; close to Curitiba, the capital of the state of Paraná) is the location of the odour source in Brazil. This site is within flat and elevated terrain. Land uses such as farmland, remaining forest, woody wetlands, low residential areas, and a few industries can be found scattered around the emission source in nearly all directions. The Austrian site is located in Groß-Enzersdorf (48.203° N, 16.564° E, 151 m ASL), district of Gänserndorf in Lower Austria, and east of Vienna. It is within mainly flat terrain, typically farmland. However, surrounding residential dwellings and a few industries (mainly in the southwesterly and southeasterly directions) are present about 350–500 m from the source.

2.2. Characterisation of the odour source

Among the sources of uncertainty in dispersion modelling, algorithms that deal with the source typology are prominent. According to Pullen and Vawda (2007), predicted concentrations are fundamentally more accurate for single stacks, first hand. So, we chose a single point source for the investigation. The odour emission rate (OER) is constant, continuous, and stationary in time, with an annual mean value of 17,500 ou_E/s. A variety of emission factors can be found in the German guideline VDI 3894 Part 1 (2011) to translate this OER into a typical livestock building. The geometry of the source is presumed circular, with a height of 6 m from the ground, inner diameter of 1.2 m, and vertical release. The exit velocity is 3.0 m/s, and the gas temperature is 35 °C. This source configuration attempts to replicate the emission from a typical mechanically ventilated livestock building. Table 1 summarises the odour source parameters assumed for the dispersion calculations.

2.3. Atmospheric dispersion modelling

The U.S. Environmental Protection Agency (U.S. EPA) regulatory air quality model, AERMOD Modelling System, was used. The model has also been adopted worldwide and accepted for regulatory demonstrations by several other environmental agencies. Essentially, the modelling system consists of three modules: the AERMOD dispersion model itself, the AERMET meteorological processor, and the AERMAP terrain processor. AERMOD is fundamentally a steady-state Gaussian plume model with algorithms based on planetary boundary layer turbulence structure and scaling concepts. AERMOD is the U.S. EPA preferred/recommended software for demonstrating regulatory compliance for short-range transport of air pollutants (<50 km), including treatment of surface and elevated sources for simple and complex terrain. The steady-state concept assumes that over the model time step, the emissions, meteorology, and other model inputs, are constant all over the modelling domain. This assumption results in a resolved plume with the emissions distributed throughout the plume according to a Gaussian distribution (U.S. EPA, 2017). Comprehensive model principles and formulation can be found elsewhere (Cimorelli et al., 2005; Perry et al., 2005; U.S. EPA, 2016a). The model is used with the graphic user interface AERMOD View 9.4.0, version 16216r (Lakes Environmental Software, Ontario, Canada). The suitability of AERMOD for the scenarios of this work is justified based on: (i) the topographic features and meteorological conditions of the areas being modelled, (ii) the detail and accuracy of the primary inputs (meteorology and emission) required for a refined model, (iii) the way complexities of atmospheric processes are handled by the model, (iv) the need to apply a recognised model typically used in the permitting process, (v) the efficiency relationship between computational time and reasonable accuracy; and finally, (vi) the resources available to apply such desktop software. The modelling protocol follows current default regulatory options consistent with the Guideline on Air Quality Models (U.S. EPA, 2017), except where stated and justified otherwise.

The modelling domain, at both sites, consists of a circular area of 750 m radius centred on the source. The domain is discretised using a uniform polar grid network. Receptors are distributed along 72 radial directions, with the initial direction at 0° and with moves of 5° clockwise, over 20 concentric rings. The nearest and the last ring are placed 50 m and 750 m from the source, respectively. The distance of the nearest ring from the source allows for the satisfactorily accurate calculation of odour concentrations because to date Gaussian plume models are inherently more uncertain for receptors very close to the source. 1440 receptor points are placed for the calculation of odour concentrations for each site. The design of the receptor network is supported by the receptor density and location and not because of the total number of receptors. The receptor grid is progressively more resolved near the source, which proves to be the hotspot of maximum impact for our scenarios (highest predicted concentrations). Both the receptor grid and the size of the modelling domain influence the computational model time. Consequently, their assumptions reflect the level of detail needed for the output. In other words, the choices capture the extent of the odour impact adequately. Receptors are positioned 1.5 m above the ground at the average height of the human nose. No background concentrations are assumed. The influence of a possible building downwash effect is not considered. Both sites are classified as rural, so the rural dispersion option was selected.

Terrain elevation data are obtained from the Shuttle Radar Topography Mission (SRTM) conducted by the National Aeronautics and Space Administration (NASA). The data for the modelling domains are in SRTM1 (spacing for individual data points is 1 arc-second), which corresponds to about 30 m resolution. Accordingly, the digital elevation models are built using the AERMAP terrain processor, version 11103 (U.S. EPA, 2016b). The modelling domain at the Brazilian site has elevations from near 883 m to 911 m ASL. For the Austrian site, elevations from near 147 to 153 m ASL can be found (Fig. 1). The model can account for elevated orographic effects. This is performed by inputting elevated receptor heights to model the effects of terrain above or below stack base.

Table 1 – Characteristics of odour source assumed for dispersion calculations.

Parameter	Description	Unit
Source type	Point	.
Release type	Vertical	.
Geometry	Circular	.
Release height	6	[m]
Inner diameter	1.2	[m]
Gas temperature	35	[°C]
Exit velocity	3.0	[m/s]
Volume flow rate	3.39	[m^3/s]
Odour emission rate	17,500	[ou_E/s]

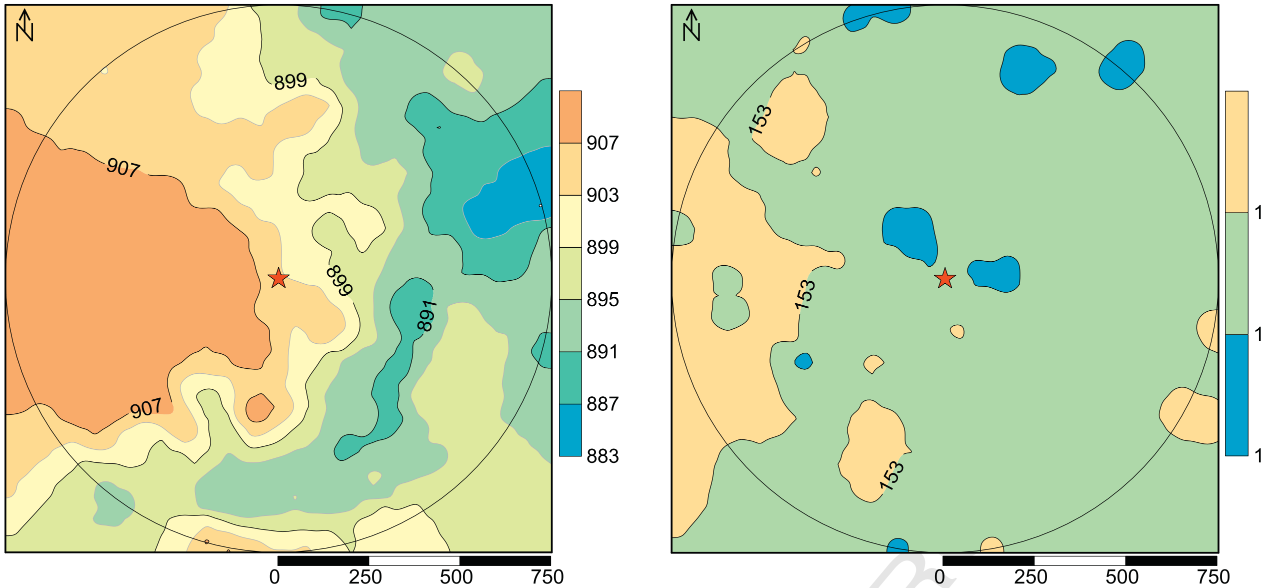

Fig. 1 – Elevations at (left) São José dos Pinhais/Brazil and (right) Groß-Enzersdorf/Austria: Modelling domains are within the circular areas of 750 m radius centred on the source (red star marker). Legends denote elevations in meters and their associated colours; scale bars indicate meters. For interpretation of the colours used in this figure, the reader is referred to the web version of this work.

Because of the orography of the sites, the elevated option is used to characterise the terrain effects. Elevations/hill heights are assigned to receptors and the odour source by AERMAP.

Land surface characteristics (i.e., albedo, Bowen ratio, and surface roughness length) around the meteorological towers were determined by the procedures of AERSURFACE (U.S. EPA, 2008) and AERMET User's Guides (U.S. EPA, 2016c) using the AERSURFACE utility (version 13016). For the Brazilian site, surface characteristics were extracted from the Global Land Cover Characterisation *GLCC* for South America, with a resolution of 1 km. For the Austrian site, the CORINE CLC2006 database with 0.1 km resolution was used. In order to improve the resolution and to homogenise the resolution of the surface characteristics data, a refinement was performed using the tool called *Land Use Creator* available for AERMOD-View. The surface roughness was determined by sectoring (12 angular sectors of 30°) with a default upwind distance of 1 km radius relative to the meteorological tower location. Albedo and the Bowen ratio values were determined based on a default area of 10 × 10 km also centred on the meteorological tower. Monthly values were assigned to account for a temporal change of surface characteristics.

The adjusted surface friction velocity technique (ADJ_U*) is currently considered a default regulatory option in the AERMOD (U.S. EPA, 2016c). As a previous diagnostic evaluation, we ran the model for both sites to verify the sensitivity that the ADJ_U* option could exert on the predicted concentrations. The model results at both sites showed high linear correlation ($R^2 \approx 0.99$) for ADJ_U* turned on against ADJ_U* turned off, for the two OIC tested (Section 1.5). Residual plots further exhibited the goodness of linear fit. Moreover, by visual scrutiny on the shape of the separation distances (contour plots), no changes in the envelope were found. Once model outputs at both sites were well-correlated for ADJ_U* turned on against ADJ_U* turned off for the selected OIC, the usage of the ADJ_U* option becomes non-compulsory for our modelling scenarios. In response, we ran the model with ADJ_U* turned off to demonstrate the full range of atmospheric stability estimated by AERMET (Section 2.2).

2.4. Meteorology

2.4.1. Brazilian site

Surface meteorological observations of 1 h time-steps for wind direction (W_d), wind speed (W_s), air temperature (T), atmospheric pressure (P_{atm}), and cloud cover (CC) were obtained from the National Oceanic and Atmospheric Administration (NOAA) database for Afonso Pena International Airport *SBCT* (−25.531° S, −49.167° W). At airports, W_d is typically recorded to the nearest 10° for that hour. The weather years selected to perform the modelling were 2004, 2008, 2013, 2014, and 2015. Due to not meeting the U.S. EPA minimum requirements of completeness, the additional annual datasets from 2005 to 2016 were disregarded. Preprocessing was conducted to fix unordered times, non-uniformly spaced times, missing data, and duplicate records. Gaps were filled using established data substitution protocols (U.S. EPA, 2000, 2016c). Representativeness regarding both spatial and temporal resolution of the meteorological data is mandatory. The SBCT station dataset is representative of the meteorological conditions at the source location and in adjacent areas because of the (i) proximity of the meteorological tower to the area being modelled: (~4.5 km), (ii) complexity of the terrain: topography between the surface station and the source location is not complex, (iii) surface characteristics: comparable land use characteristics around the meteorological tower to the area being modelled, and (iv) period of the data collection and completeness: recent and valid years of weather data are used. Upper air data for the weather years previously selected were obtained for SBCT from the NOAA/ESRL Radiosonde Database. Both surface and upper air data were inspected using quality assurance procedures and validation and were processed using AERMET (version 16216). Atmospheric pressure is used within the model basically to calculate dry air density, and cloud cover is a necessary input to AERMET to derive the micrometeorological parameters. The model uses the Monin-Obukhov similarity theory to estimate the stability of the planetary boundary layer. This theory is grounded on the Obukhov stability length, which is an estimation of the height where the shear production of turbulent kinetic energy is comparable with the buoyancy production of turbulence kinetic energy (Temel and van Beeck, 2017).

2.4.2. Austrian site

Primary surface meteorological data in 1 h time-steps for W_d, W_s, T, and P_{atm} were made available by the Central Institute for Meteorology and Geodynamics (ZAMG, Vienna, Austria) for Groß-Enzersdorf GE (48.199° N, 16.559° E). Wind direction was recorded to the nearest 1°. However, GE station does not have CC observations; then, this variable was also provided by ZAMG for Schwechat Vienna International Airport LOWW (48.110° N, 16.569° E) which is situated ~10 km from the source. Minor missing data were filled using recommended procedures. The period of data collection is associated with the Brazilian site to harmonise the meteorological years used for model calculations. For that reason, we selected five years of weather data for each site. The GE station dataset is representative of the spatial and temporal conditions at the odour source location and in adjacent areas for the same conditions previously described (e.g., the meteorological tower is located ~0.6 km from the source). Upper air data for the corresponding surface weather years were obtained from the NOAA/ESRL Radiosonde Database for Wien-Hohe Warte WHW (located ~16 km from the source, 48.248° N, 16.356° E).

Table 2 summarises the information on the surface and upper air meteorological stations at the Brazilian and Austrian sites.

2.5. Selection of odour impact criteria

The calculation of the direction-dependent separation distances was performed for two national OIC, as follows:

- OIC_1: $C_t = 0.25\ ou_E/m^3$, P = 90th, $A_t = 1$ h;
- OIC_2: $C_t = 1\ ou_E/m^3$, P = 98th, $A_t = 1$ h.

The OIC_1 is presently used in Germany (GOAA, 2008; TA-Luft, 2002). The OIC_2 is used, for example, in Flanders (Belgium) for new geographically isolated livestock farms (LNE, 2008; Willems et al., 2015). Criteria of this type are often used for odour impact assessment purposes. A detailed description of OIC in several jurisdictions throughout the world can be found in recently published papers (Brancher et al., 2017; Brancher et al., 2016; Sommer-Quabach et al., 2014).

For all simulations, the same source data and modelling assumptions were considered. This arrangement enables the calculated separation distances to deviate mainly because of the length of the meteorological input data and the selected OIC. Meteorological data were combined into a single model run encompassing the whole period of meteorology (i.e., multiple-year modelling configured by concatenating the five individual years of meteorological data for each site). The results of these multiple-year model runs were named "5 years". Furthermore, individual model runs were conducted for each meteorological year separately. In this case, each output was named according to the year in which the meteorological data collection occurred.

2.6. Statistical analysis

Separation distances are typically drawn to the opposite side of the W_d because this is the direction to which emissions spread. This direction is called transport direction T_d (given by $T_d = W_d + 180°$). For instance, when the wind blows from the South (180°) the corresponding separation distance is located to the North (T_d of 360°) (Schauberger et al., 2006; VDI 3894 Part 2, 2012). The calculated direction-dependent separation distances are given in increments of 10° using the stack position as the reference point for the distance determination. The separation distances are given in full meters. The contour method used to draw the separation distances is B-spline

Table 2 – Meteorological stations selected for the modelling applications. The meteorological years used are 2004, 2008, 2013, 2014, and 2015.

Site	Station code	Type	Coordinates	Elevation ASL (m)	Distance from the source (km)	Hourly meteorological parameters
Brazil	SBCT	Surface	−25.531° S, −49.167° W	908	4.5	W_d, W_s, T, P_{atm}, CC
	SBCT	Upper air	−25.531° S, −49.167° W	908	4.5	W_d, W_s, T, P_{atm}
Austria	GE	Surface	48.199° N, 16.559° E	154	0.6	W_d, W_s, T, P_{atm}
	LOWW	Surface	48.110° N, 16.569° E	183	10	CC
	WHW	Upper air	48.248° N, 16.356° E	198	16	W_d, W_s, T, P_{atm}

SBCT: Afonso Pena International Airport; GE: Groß-Enzersdorf; LOWW: Schwechat Vienna International Airport; WHW: Wien-Hohe Warte; W_d: wind direction; W_s: wind speed; T: air temperature; P_{atm}: atmospheric pressure; CC: cloud cover; ASL: above sea level.

Please cite this article as: Brancher, M., et al., Assessing the inter-annual variability of separation distances around odour sources to protect the residents from odour annoyance, J. Environ. Sci. (2018), https://doi.org/10.1016/j.jes.2018.09.018

smoothing. Statistical analyses were performed using the Guide to the expression of Uncertainty in Measurement (GUM), which recommends a standardised approach for expressing the uncertainty of measurements (BIPM et al., 2008). We determined the mean separation distance values (sample size = 5), the standard deviations (degrees of freedom = 4), in addition to the upper and lower confidence interval boundaries (k = 2, level of confidence = 95%) over the single meteorological years. The coefficient of variation CV, which is defined as the standard deviation divided by the mean with the result reported as a percentage, is used to show the extent of variability in relation to the mean separation distance values over the individual meteorological years. The CV is widely used in many fields when performing quality assurance and evaluations of repeatability and reproducibility. We also compared the direction-dependent separation distances for the model runs using the five years of meteorological data against the distances resulting from single meteorological years, in addition to the mean values over the single meteorological years.

3. Results

3.1. Surface meteorological conditions

The wind statistics for the Brazilian site (São José dos Pinhais, SBCT station) shows that the prevailing wind during the five years of meteorological observations (2004, 2008, 2013–2015) is East to Southeast (E–SE). Winds characterised as calms (< 0.5 m/s) amount to ~3.5% of the observations. The average W_s is 3.3 m/s; high speeds can be experienced from nearly all directions, with a maximum of 25.7 m/s for the period. The site is located on a plateau ~0.9 km ASL hence low atmospheric pressure is observed (915 hPa, on average). The site altitude and location also result in monthly mean temperatures being mild in the summer and relatively cold during the winter.

Groß-Enzersdorf in Austria can have high wind speeds, mainly from prevailing northwesterly (NW) directions, during the selected meteorological period. The secondary prevailing wind direction is from Southeast (SE), which also can have stronger winds. Whereas the northwesterly wind is mainly associated with cloudy or rainy periods, the southeasterly wind is regularly observed with anticyclonic conditions. Calm winds account for approximately 0.4% of the observations. The average W_s is 3.3 m/s; the highest speed of the period is 13.2 m/s. In general, the weather conditions for Groß-Enzersdorf are characterised by different seasons regarding temperature. The winter has relatively low monthly mean temperatures, while in summer high monthly mean temperatures are observed.

For both sites, calm conditions recorded in the surface meteorological dataset are not excluded for dispersion calculations. The calms are adjusted into a minimum speed threshold of 0.5 m/s and uniformly redistributed around the compass to maintain the wind profile. However, this inclusion is considered minor because 3.5% and 0.4% of the total hours were added for the Brazilian and Austrian datasets, respectively. Table 3 shows the descriptive statistics for hourly mean values of the two meteorological datasets over the five years at the Brazilian and Austrian sites, respectively. Fig. 2 and Fig. 3 show the annual wind roses with distributions of wind direction for 10° sectors (i.e., 36-part wind roses) at the Brazilian and Austrian sites, respectively. While the general characteristics are preserved, a distinctive year-to-year variation in the wind data can already be delineated from a visual inspection of these figures.

3.2. Atmospheric stability

The Obukhov length L, with dimension of length (m), is used by AERMET to estimate the atmospheric stability. Here, we show L as an indicator of atmospheric stability estimated by the model, and not as a definitive measure of the dispersion of the plume. Because L, by definition, can approach positive or negative infinity for neutral states, the inverse of L (1/L, given in m^{-1} and often called the Obukhov stability parameter) is assessed. Unstable atmospheres have negative values of 1/L; neutral atmospheres have |1/L| values of approximately zero; stable atmospheres have positive values of 1/L. Consequently, the more positive the 1/L value, the greater the atmospheric stability is assumed to be. Similarly, the more negative 1/L becomes, the more unstable the surface layer is presumed.

Once we turn off the ADJ_U* option for the modelling applications, the maximum and the minimum of L that can be calculated by the model are +1 m and − 1 m, respectively. Consequently, the magnitude of the 1/L values (per meter) is within this interval. Fig. 4 presents bivariate histogram plots to show the atmospheric stability (given by 1/L) estimated by AERMET against wind direction and speed. On the top panel of Fig. 4, the stability is shown for the Brazilian site and on the bottom panel for the Austrian site. These charts cover five years of meteorology data (2004, 2008, 2013, 2014, and 2015) at both sites.

The dependence of turbulence on the wind speed is confirmed, as expected. With increasing wind speed, there is a tendency that only near-neutral conditions for both sites occur. At both sites, neutral stability essentially dominates with wind speeds greater than ~5 m/s. Extremely unstable and moderately stable atmospheric conditions are both estimated for very low wind speeds (<1.0 m/s). For example, greater abundance of extremely unstable conditions with 1/L

Table 3 – Descriptive statistics for hourly meteorological surface observations used for the model calculations according to the period of data collection.

Parameter	Station	Minimum	Maximum	Mean
Wind speed (m/s)	SBCT	0.5	25.7	3.3
	GE	0.5	13.2	3.3
Temperature (°C)	SBCT	−3.0	33.0	17.4
	GE	−16.5	38.0	11.4
Atmospheric pressure (hPa)	SBCT	900	930	915
	GE	959	1029	998
Cloud cover (tenths)	SBCT	0	10	7.6
	GE	0	10	6.7

SBCT: Afonso Pena International Airport; GE: Groß-Enzersdorf.

Please cite this article as: Brancher, M., et al., Assessing the inter-annual variability of separation distances around odour sources to protect the residents from odour annoyance, J. Environ. Sci. (2018), https://doi.org/10.1016/j.jes.2018.09.018

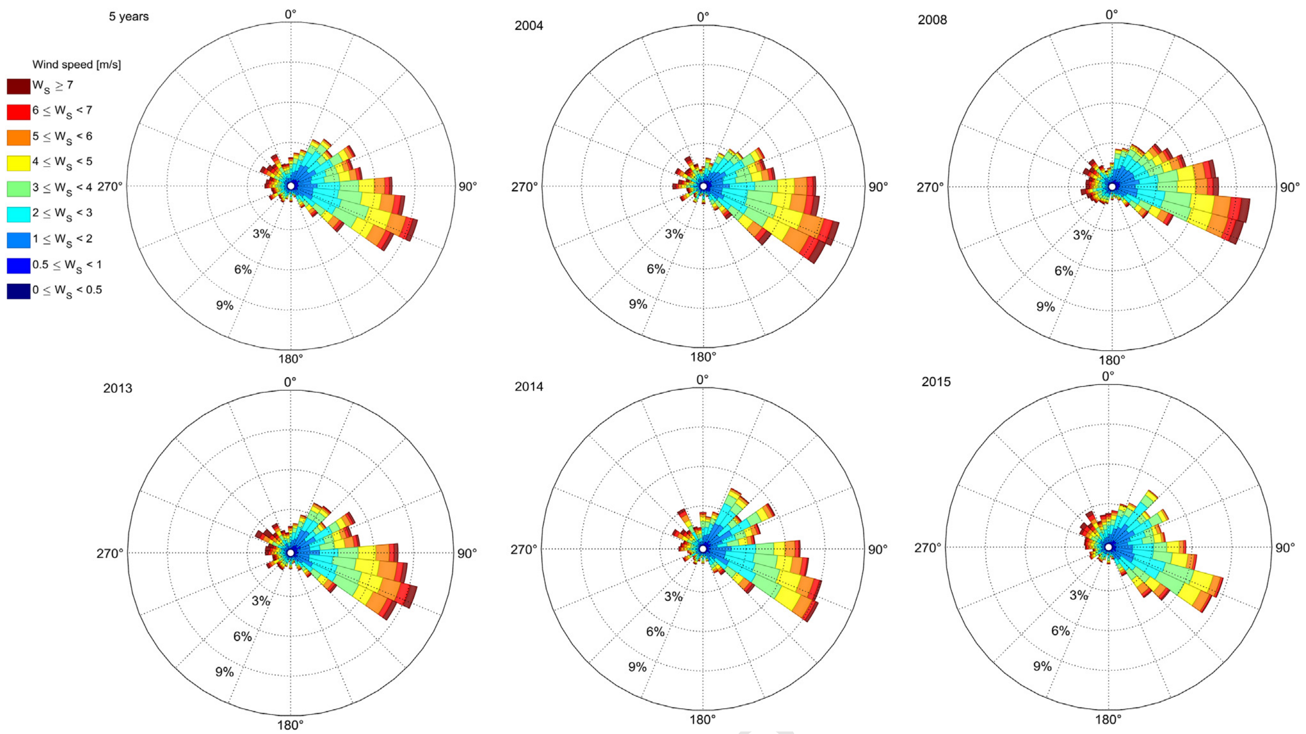

Fig. 2 – Wind roses at São José dos Pinhais (SBCT station, Brazil): Legend denotes wind speed categories and their associated colours. For interpretation of the colours used in this figure, the reader is referred to the web version of this work. W_S: wind speed.

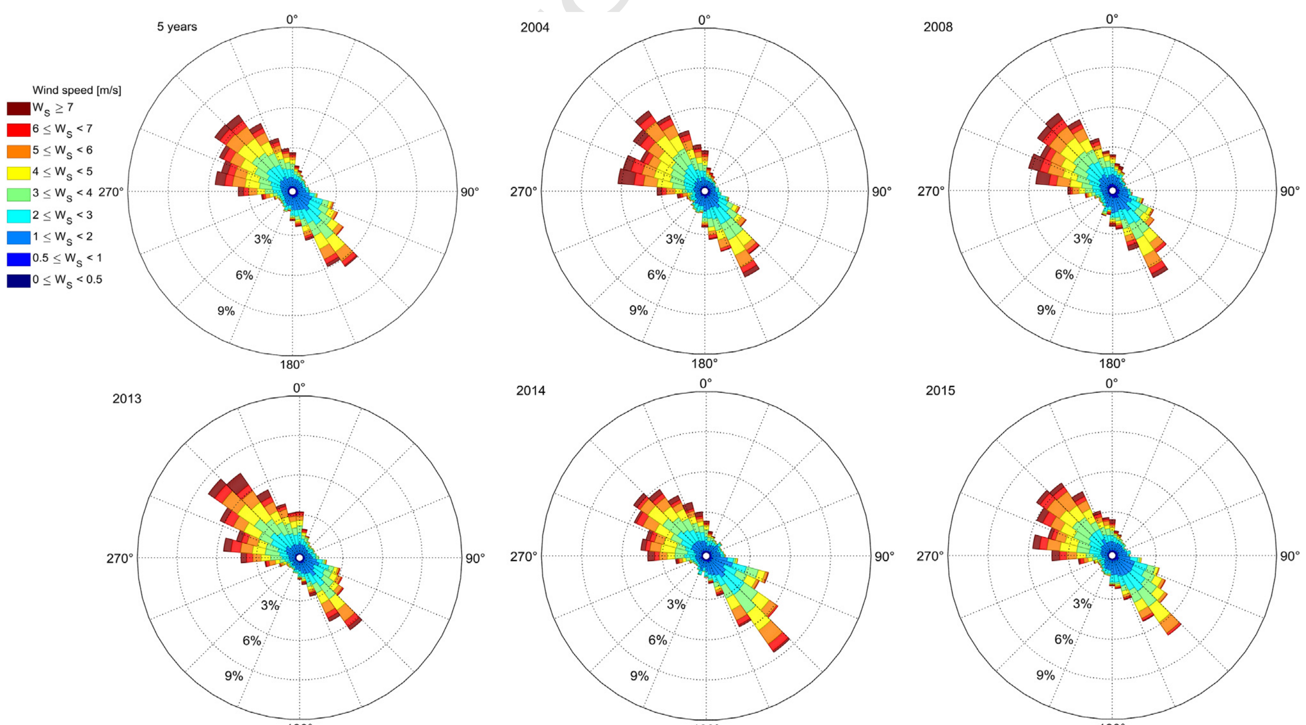

Fig. 3 – Wind roses at Groß-Enzersdorf (GE station, Austria): Legend denotes wind speed categories and their associated colours. For interpretation of the colours used in this figure, the reader is referred to the web version of this work. W_S: wind speed.

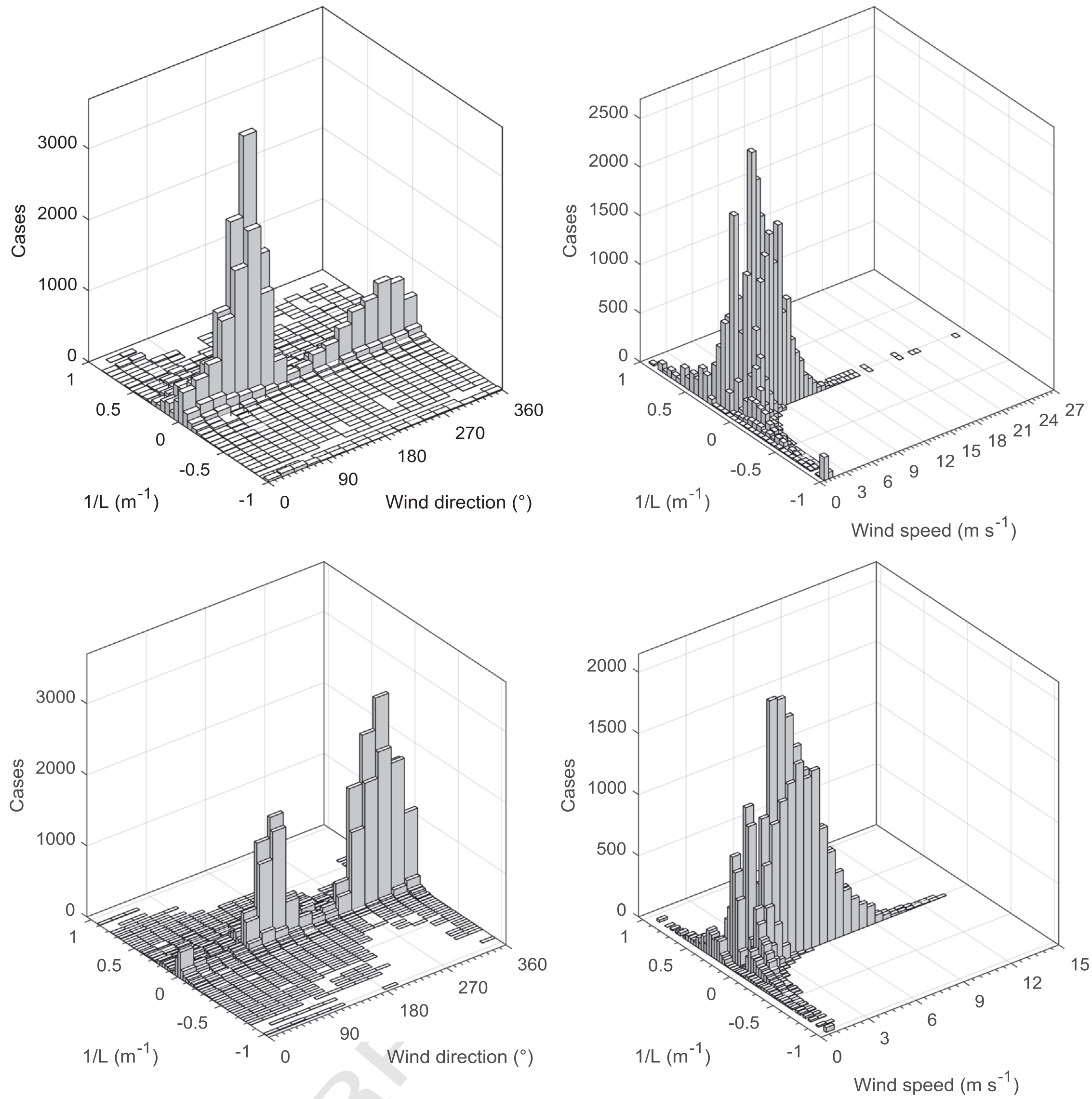

Fig. 4 – Obukhov stability parameter estimated by AERMET against wind direction and speed at (top) São José dos Pinhais/Brazil and (bottom) Groß-Enzersdorf/Austria. Meteorological data for years: 2004, 2008, 2013, 2014, and 2015. 1/L: Obukhov stability parameter.

values of −1.0 m^{-1} at the Brazilian site (302 cases, 0.7% of the total observations), and with wind from numerous directions, are observed than at the Austrian site (40 cases, 0.1% of the total observations). These extremely unstable conditions are only associated with certain wind directions.

Also, an effect by which low wind speeds favoured the incidence of daytime unstable and night-time stable atmospheric conditions, is detected at both sites. Plots of the annual Obukhov stability parameter 1/L against wind direction and speed (data not shown) indicate that the atmospheric stability (estimated by AERMET) is similar among the years at each site. Some year-to-year differences can be observed, mainly for the dependence on the wind direction. The inter-annual variability of the atmospheric stability appears to be lower than for the wind data, whereby the Brazilian site shows more variation than the Austrian site.

3.3. *Direction-dependent separation distances*

Fig. 5 shows the direction-dependent separation distances measured in increments of 10° at São José dos Pinhais (Brazil) and Groß-Enzersdorf (Austria). The results for OIC_1 are shown on the left panels and for OIC_2 on the right panels.

Considerable differences in the shape, length, and transport directions T_d are found between the sites. These differences are, evidently, due to the yearly varying meteorological conditions at each site, once the same source data and modelling assumptions are considered for all modelling runs.

The distribution of W_d primarily drives the spreading of the separation distance. This is made clear by comparing wind roses (Figs. 2 and 3) with the shape of the separation distance at the Brazilian and Austrian sites (Fig. 5). The largest distances are observed in the prevailing wind

Please cite this article as: Brancher, M., et al., Assessing the inter-annual variability of separation distances around odour sources to protect the residents from odour annoyance, J. Environ. Sci. (2018), https://doi.org/10.1016/j.jes.2018.09.018

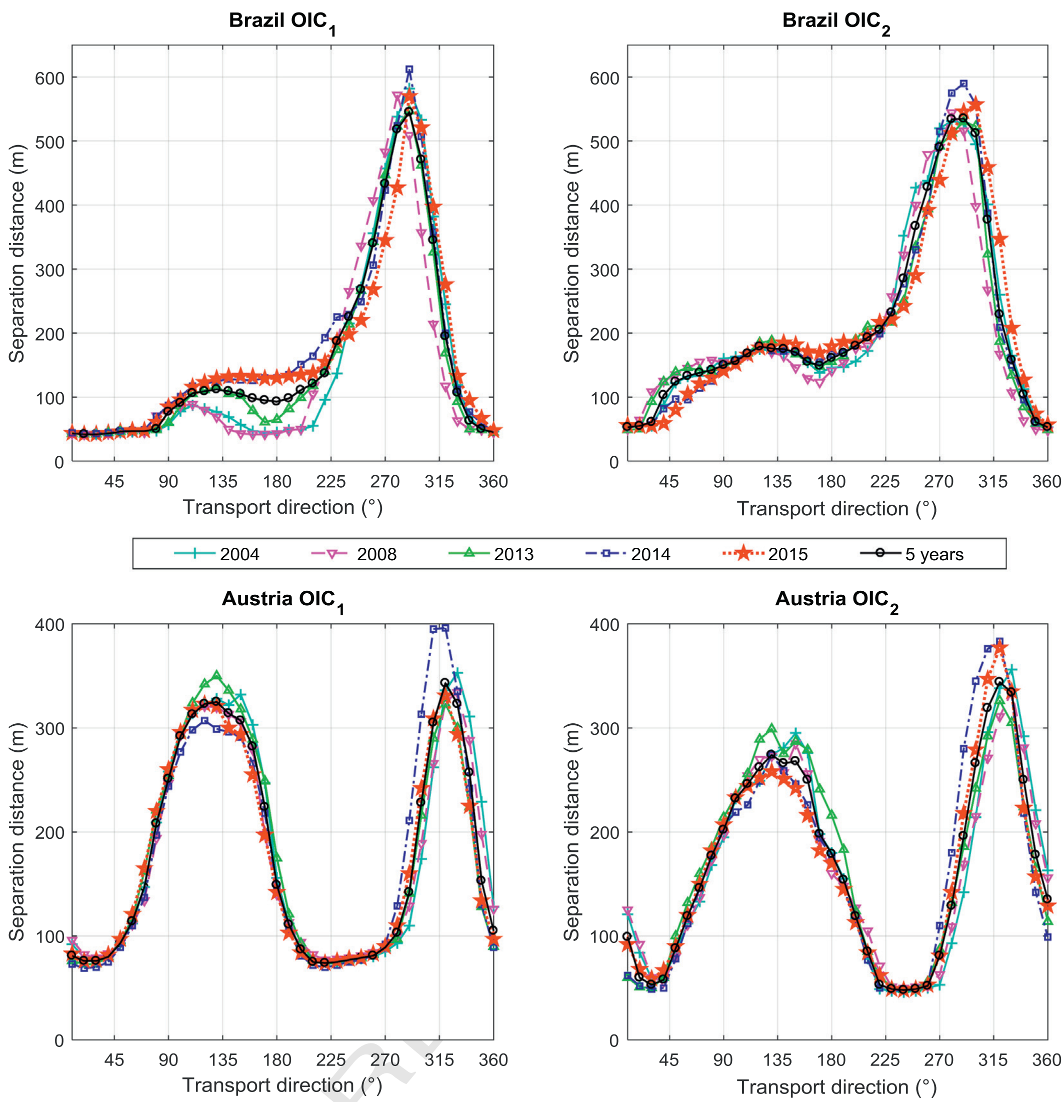

Fig. 5 – Direction-dependent separation distances at the Brazilian and Austrian sites: Legend denotes the meteorological years used for the model calculations and their associated colours and markers. OIC: odour impact criteria.

directions. Accordingly, a priori one can expect that the higher the frequency of a certain wind direction sector, the greater the elongation of the separation distance will be in that direction. However, the extent of the distances is probably a combination of many factors such as the frequency distribution of atmospheric stability classes and wind speeds per wind direction sector, as well as the selection of the OIC.

At the Brazilian site, a maximum separation distance of 612 m and 590 m for the OIC_1 and OIC_2 are obtained, respectively. These distances occur at $T_d = 290°$ in 2014. The minimum separation distance in $T_d = 290°$ is 547 m for the OIC_1 (in 2013) and 528 m (in 2004). The minimum separation distance considering all wind direction sectors is 42 m for the OIC_1 and 49 m for the OIC_2 at north-easterly T_d, with almost no variation from year to year. The highest variation of separation distance from one year to the next at the Brazilian site is observed for the OIC_1 in the sector from 140° to 210°. Another source of inter-annual variability occurs for the OIC_2 between 30° and 60°. Both scenarios of odour criteria also have year-to-year variations in the prevailing wind. All in all, a variation in T_d between ~ 50 and 600 m is observed at the Brazilian site.

At the Austrian site, two main separation distance peaks are observed around the odour source because of the prevailing winds heading in these directions. For the OIC_1, a maximum separation distance of 396 m for $T_d = 320°$ in 2014 and 350 m for $T_d = 130°$ in 2013 are found. Using OIC_2 results at a maximum separation distance of 383 m for $T_d = 320°$ in 2014, and 299 m for $T_d = 130°$ in 2013. The minimum separation distance in the prevailing winds is 323 m for a $T_d = 320°$ in 2013 and 307 m for a $T_d = 120°$ in 2013 for the OIC_1. Considering OIC_2, a minimum separation distance in the prevailing winds of 326 m for a $T_d = 320°$ in 2013 and 258 m for a $T_d = 130°$ in 2015 are obtained. At the Austrian site, the largest variations of separation distance from year to year are observed mainly in the prevailing winds for both OIC_1 and OIC_2. All in all, separation distances vary in T_d between ~ 50 and 400 m at the Austrian site.

3.4. Inter-annual variability of the direction-dependent separation distances

For evaluating and expressing the amount of inter-annual variability in the direction-dependent separation distances, we present Fig. 6. At both sites, the mean direction-dependent separation distances over the individual meteorological years are largely in agreement with the distances determined for the five years of meteorology data. This result can be observed in Fig. 6 through the great overlapping of the lines “mean over single years” and “5 years”. Moreover, the separation distances determined for the five years of meteorology, assumed herein as the “true value”, are continuously inside the confidence interval of the mean direction-dependent separation distance values determined for the individual years of meteorology data.

As previously identified, the peak of variability at the Brazilian site is for a sector between 140° to 210° when selecting the OIC_1 to delineate the distances. In this regard, a CV of about 55% is observed for Td = 170°. For the OIC_2, a CV of 34% is determined for a T_d of 30°. The overall CV for all direction-dependent distances corresponds to 21% and 12% for the OIC_1 and OIC_2, respectively.

At this point, the question arises as to why the results at the Brazilian site have high variation of separation distances from year to year in some specific directions. Wind data analysis shows a time trend for particular wind direction sectors. In this analysis, the slope k1 for linear regression of the wind frequency data is calculated. The prevailing wind directions (~50 to 110°) show a negative slope for the trend of the wind frequency, whereas the wind directions between ~280 and 50° shows district positive slope. In between these

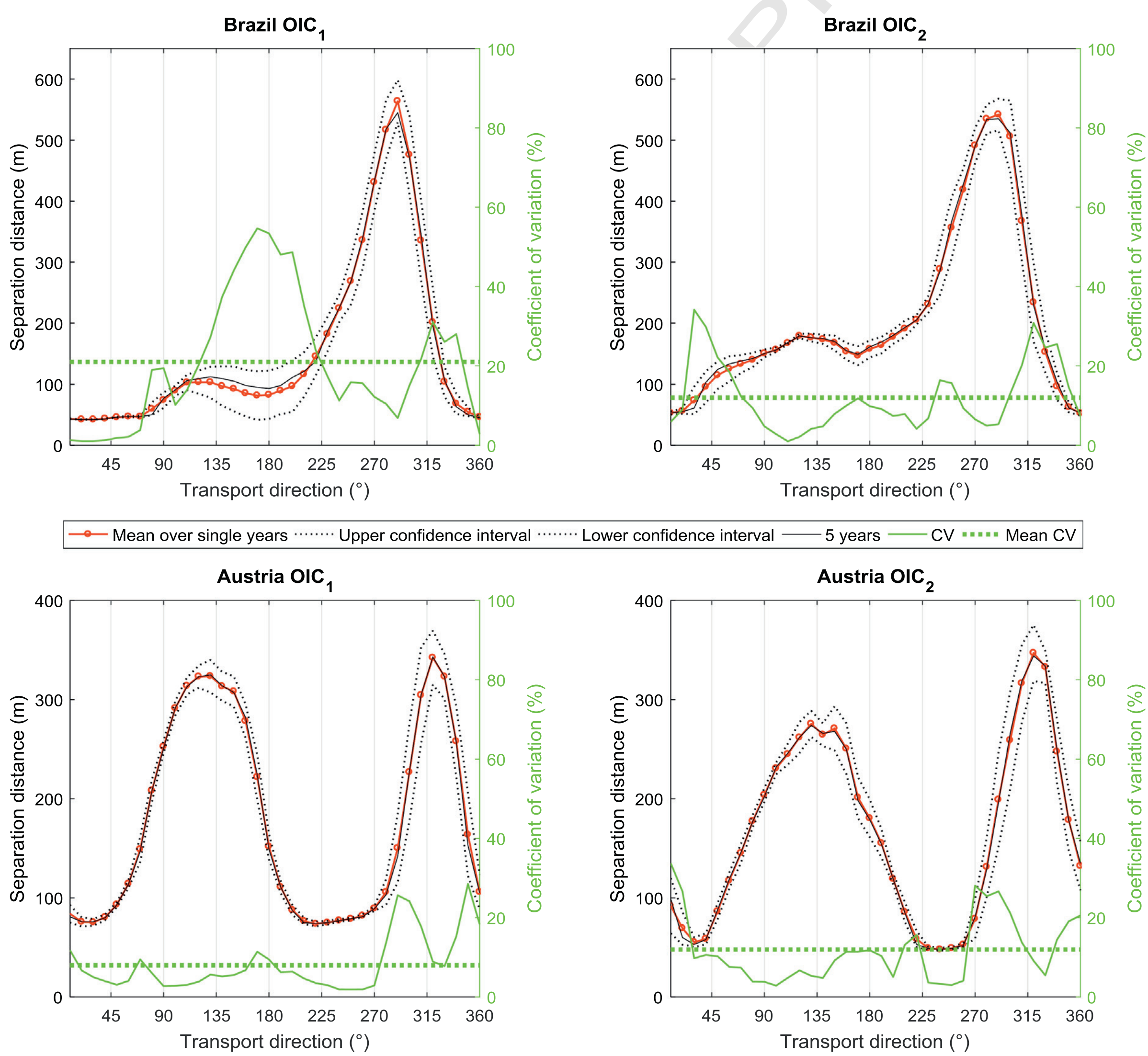

Fig. 6 – Inter-annual variability of the direction-dependent separation distances at the Brazilian and Austrian sites. Legend denotes the metrics used for the evaluation. OIC: odour impact criteria; CV: coefficient of variation.

two regions no time trend is detected. This means that the prevailing wind directions become less frequent, while the wind frequency for the sector between ~280° and 50° is increasing. The relative trend in % (given by k1 divided by the mean value of the wind direction frequency for each sector) is also calculated. It is observed high values for the relative trend between ~ 350° and 40° with an increase of about 3 to 5% per year, which is more than the relative trend for the other wind directions. This can be considered as a systematic error rather than a random error. Therefore, the relative trend further explains that the wind frequency for the period of meteorology herein used is increasing for this sector which is related to the high variation of the annual separation distances.

At the Austrian site, some peaks of variation in the annual separation distances are observed for both OICs. However, these peaks are not very pronounced. This reflects the overall CV for all direction-dependent distances of 8% and 12% for OIC_1 and OIC_2, respectively.

4. Discussion

In this work, we assessed the inter-annual variability of direction-dependent separation distances to avoid odour annoyance. The model calculations were undertaken for one site located in São José dos Pinhais (Brazil) and another in Groß-Enzersdorf (Austria). Model outputs are typically related to a specific odour impact criterion, which is a combination of an odour concentration threshold C_t, a percentile rank value P, and an averaging time A_t. Here, two typical national OIC were selected to calculate the separation distances as a final measure of the expected odour annoyance (Section 1.5). The comparability of the two national OIC was shown by Sommer-Quabach et al. (2014).

The same emission characteristics and modelling assumptions were used for both sites. This means that the outcomes are largely dependent on the site meteorology and the selected OIC. We collected, preprocessed and validated five years' time-series of hourly meteorological observations for each site. São José dos Pinhais, near Curitiba, can experience high wind speeds from nearly any direction. The prevailing wind blows from between E and SE. Fig. 2 shows some inter-annual variability, especially in the main wind directions, both concerning the frequency of occurrence and to the wind speed. Groß-Enzersdorf, in Lower Austria east of Vienna, can have high wind speeds mainly from NW directions. The secondary prevailing wind directions are from SE, directions which can have stronger winds as well. In contrast to the Brazilian site, Groß-Enzersdorf shows the bi-polar structure of wind directions commonly observed in Central Europe, attributable to the west wind belt at these latitudes with alternating low and high-pressure influence. Inter-annual variability in the wind data here appears to be lower than at the Brazilian site when comparing Figs. 2 and 3. For both sites, the average W_s is 3.3 m/s, and the terrain within the modelling domain is in large part flat, with some receptors located in elevated positions.

As far as atmospheric stability is concerned, the Brazilian site is subjected to more unstable conditions than the Austrian site (Fig. 4). This is expected because of the climate classification of the sites, which further endorses the approach selected to determine atmospheric stability via the Obukhov length L. With increasing wind speed, neutral conditions are predominant at both sites.

The meteorological conditions, especially the distribution of wind directions, are reflected in the direction-dependent separation distances (Fig. 6). Both the range and the inter-annual variability of the separation distances are larger at the Brazilian than at the Austrian site. The separation distances vary over the transport direction T_d between ~50 and 600 m at São José dos Pinhais and 50 to 400 m at Groß Enzersdorf.

At São José dos Pinhais, OIC_2 often delivers larger separation distances than did OIC_1, whereas, at Groß-Enzersdorf, OIC_1 often delivers the larger separation distances. This is the combined effect of the wind speed and stability data for each wind direction sector. The maximum separation distances of about 600 m for a T_d = 290° at the Brazilian site, for example, result from a combination of a high frequency of the relevant T_d, high wind speeds and a large amount of neutral to slightly stable atmospheric stability.

From the short interpretation of meteorological data given before, it is no surprise that the inter-annual variability of the separation distances is generally larger at São José dos Pinhais than at Groß-Enzersdorf (Figs. 5 and 6). At both sites, a dependence on the transport direction can be seen that is different between the two OIC used. At the Brazilian site, the largest CV is obtained for the seldom occurring southerly T_d for OIC_1. At Groß-Enzersdorf, the CV is often high for T_d between 270° and 360°, but not inevitably for the most frequent directions.

The present work allows answering two research questions regarding the inter-annual variability of the direction-dependent separation distances, as follows.

i. *Is one year of meteorological observations enough to calculate reliable separation distances?*

In general, a fair agreement is observed between the calculated separation distances (Fig. 5). Therefore, based on the shape of the distances and the distance measurements as well as the inter-annual general tendencies (Fig. 6), a one-year dataset of hourly meteorological observations is enough to be taken as a plausible length of time to attain reliable distances. This finding is further supported because the meteorological conditions for the Brazilian and Austrian sites have no excessive dissimilarities within a period of 11 years (from 2004 to 2015), as demonstrated in the annual wind roses in addition to the atmospheric stability. Although some meteorological years were disregarded because of modelling requirements, these and other years were investigated, mainly regarding wind distribution. We observed that these data are also representative of the climatic conditions of the two sites, and of the ability of the individual parameters to characterise the transport and dispersion conditions in the areas of interest (U.S. EPA, 2017).

As noted by Featherston et al. (2014), conducting a modelling study against each meteorological year assessed independently has the effect of increasing the effective compliance threshold above the current percentile predicted odour level. In other words, a requirement for odour assessments to be conducted for individual years, and compliance obtained for each of these individual years, increases the percentile that an odour source must comply with for licencing. Furthermore, Featherston et al. (2014) state that applying in particular the 99.9th percentile across the meteorological dataset as a whole is more representative of real-world dispersion because significant smoothing of the petal/fingering pattern (usually associated with Gaussian plume model plots) was observed.

Bear in mind, the Guideline on Air Quality Models (U.S. EPA, 2017) accepts at least one year of “site-specific” meteorological data for conventional air pollutants. Also, this guide states that if more years are available, more data is preferred for use in air quality analyses, which is rational. The data from the most recent and valid meteorological year should be preferred, according to international modelling guidelines. This recommendation is mainly related to possible changes in the surface roughness around meteorological towers over the years, which might influence local micrometeorology patterns.

Regarding policy implications, in many countries, the use of more than one year of meteorological data for odour dispersion modelling is mandated. One year is accepted in a few other countries (Brancher et al., 2017). However, lacking a sound scientific basis for odour. The utilisation of one single year of meteorological data has the potential to improve the relationship between accuracy and time/financial resources in odour modelling studies, and aid harmonisation of odour modelling guidelines.

ii. *Which inter-annual variability can be expected if one year of meteorological observations is used to calculate direction-dependent separation distances?*

Significant volatility within the separation distance results from one year to the next is not observed at the two sites under investigation. If a single year of meteorology is reasonable to calculate separation distances to avoid odour annoyance, the amount of inter-annual variability involved in this outcome arises. The mean CV values for all direction-dependent distances at the Brazilian site correspond to 21% and 12% for the OIC_1 and OIC_2, respectively. At the Austrian site, the mean CV values for all direction-dependent distances are 8% and 12% for OIC_1 and OIC_2, respectively.

Therefore, the statistical analyses reveal a relatively low yearly variability, which is further evidence supporting the representativeness of one single meteorological year. The results show good agreement (Fig. 6) of the separation distances determined for the individual years of meteorology because the distances for the five years of meteorology are continuously within the confidence interval of the mean values over the single meteorological years. As previously mentioned, visual interpretation of the separation distance results (Fig. 5) also indicates the representativeness of the single meteorological years against the full five years of meteorology.

The year-to-year variation of the separation distances is most likely related to the frequency of wind direction and atmospheric stability in a certain sector. As noted by Piringer et al. (2016), the combination of atmospheric stability with frequent wind directions can be significant for large separation distances. In a comparison of separation distances at other sites across Austria, Piringer et al. (2016) showed that separation distances are a result of a complex interaction of wind conditions, stability classes, and attenuation curves due to peak-to-mean factors. As a consequence, it can be expected that these factors also will influence the year-to-year variability of separation distances. The results of the present work allow adding that such inter-annual variability can be affected by the application of the OIC. Lower percentiles (e.g., the 90th percentile) may be better at reducing inter-annual variability in the separation distances. This is because the odour concentration values related to the 90th percentile reflect commonly occurring meteorology (Schauberger et al., 2006). In contrast, odour concentration values related to very high percentiles, such as the 99.9th, have the potential to reflect more unusual meteorological conditions (ERM, 2012). Although the remarks presented in this paragraph are broadly consistent, they are not incontestable. Further research is necessary to explore the main factors driving the inter-annual variability of direction-dependent separation distances.

5. Conclusions

To the extent of our knowledge, this is the first comprehensive study to assess the inter-annual variability of direction-dependent separation distances between odour sources and residential areas to avoid odour annoyance. The results show that one single year of hourly meteorological observations is a good compromise to achieve reliable accuracy when calculating separation distances. The inter-annual variability of the separation distances is shown to be within a plausible range, which justifies this length of one year of meteorological data. Furthermore, the results indicate that long time series of meteorological data can be seen as a gold standard. However, long time-series of meteorology data are not always available, and it can be costly to prepare a large dataset to input into a dispersion model. Therefore, the findings of this study provide a meaningful step forward for odour dispersion modelling. The search for consistent separation distances that are calculated using short periods of meteorological data represents a new direction for odour modelling.

Acknowledgements

This work was supported by the Coordenação de Aperfeiçoamento de Pessoal de Nível Superior (CAPES, Ministry of Education, Brazil), within the Programa Geral de Cooperação Internacional (PGCI, No. 88881.117633/2016-01). We also would like to thank Erwin Petz and Erwin Polreich from Zentralanstalt für Meteorologie und Geodynamik (ZAMG) for the assistance with the meteorological dataset from Groß-Enzersdorf. Q7

Please cite this article as: Brancher, M., et al., Assessing the inter-annual variability of separation distances around odour sources to protect the residents from odour annoyance, J. Environ. Sci. (2018), https://doi.org/10.1016/j.jes.2018.09.018

REFERENCES

BIPM, IEC, IFCC, ILAC, ISO, IUPAC, IUPAP, OIML, 2008. Evaluation of measurement data — Guide to the expression of uncertainty in Measurement JCGM 100:2008, GUM 1995 with minor corrections. First edition; September 2008.

Blanes-Vidal, V., 2015. Air pollution from biodegradable wastes and non-specific health symptoms among residents: direct or annoyance-mediated associations? Chemosphere 120, 371–377.

Blanes-Vidal, V., Bælum, J., Nadimi, E.S., Løfstrøm, P., Christensen, L.P., 2014. Chronic exposure to odorous chemicals in residential areas and effects on human psychosocial health: Dose–response relationships. Sci. Total Environ. 490, 545–554.

Brancher, M., Schauberger, G., Franco, D., De Melo Lisboa, H., 2016. Odour Impact Criteria in South American Regulations. CET 54, 169–174.

Brancher, M., Griffiths, K.D., Franco, D., De Melo Lisboa, H., 2017. A review of odour impact criteria in selected countries around the world. Chemosphere 168, 1531–1570.

Brinkmann, T., Both, R., Scalet, B.M., Roudier, S., Sancho, L.D., 2018. JRC Reference Report on Monitoring of Emissions to Air and Water from IED Installations, Industrial Emissions Directive 2010/75/EU (Integrated Pollution Prevention and Control). European Commission. Joint Research Centre.

Campbell, J.M., 1983. Ambient Stressors. Environ. Behav. 15, 355–380.

Cantuaria, M.L., Løfstrøm, P., Blanes-Vidal, V., 2017. Comparative analysis of spatio-temporal exposure assessment methods for estimating odor-related responses in non-urban populations. Sci. Total Environ. 605-606, 702–712.

Capelli, L., Sironi, S., Del Rosso, R., Guillot, J.-M., 2013. Measuring odours in the environment vs. dispersion modelling: A review. Atmos. Environ. 79, 731–743.

Cimorelli, A.J., Perry, S.G., Venkatram, A., Weil, J.C., Paine, R.J., Wilson, R.B., Lee, R.F., Peters, W.D., Brode, R.W., 2005. AERMOD: A dispersion model for industrial source applications. Part I: General model formulation and boundary layer characterization. J. Appl. Meteorol. 44, 682–693.

De Melo Lisboa, H., Guillot, J.-M., Fanlo, J.-L., Le Cloirec, P., 2006. Dispersion of odorous gases in the atmosphere — Part I: Modeling approaches to the phenomenon. Sci. Total Environ. 361, 220–228.

Drew, G.H., Smith, R., Gerard, V., Burge, C., Lowe, M., Kinnersley, R., Sneath, R., Longhurst, P.J., 2007. Appropriateness of selecting different averaging times for modelling chronic and acute exposure to environmental odours. Atmos. Environ. 41, 2870–2880.

ERM, 2012. Environmental Resources Management. Broiler Farm Odour Environmental Risk Assessment - Background to Technical Guidance. Environmental Protection Authority of Victoria, Docklands, p. 65 ERM, Reference: 0164677.

Featherston, D., Pollock, T., Power, M., 2014. Odour Dispersion Modelling of Meat Chicken Farms: Comparison of AERMOD, AUSPLUME and CALPUFF models. RIRDC Publication No. 14/102. RIRDC Project No. PRJ-009544. Rural Industries Research and Development Corporation, p. 84.

Ferrero, E., Mortarini, L., Purghè, F., 2017. A simple parametrization for the concentration variance dissipation in a Lagrangian single-particle model. Bound. Layer Meteorol. 163, 91–101.

GHD, 2015. Odour Amenity Buffer Assessment Using AERMOD. Australian Paper Maryvale, p. 25.

GOAA, 2008. Guideline on Odour in Ambient Air GOAA. Detection and Assessment of Odour in Ambient Air Second Version, Berlin, Germany.

Griffiths, K.D., 2014. Disentangling the frequency and intensity dimensions of nuisance odour, and implications for jurisdictional odour impact criteria. Atmos. Environ. 90, 125–132.

Hayes, J.E., Stevenson, R.J., Stuetz, R.M., 2014. The impact of malodour on communities: a review of assessment techniques. Sci. Total Environ. 500–501, 395–407.

Henshaw, P., Nicell, J., Sikdar, A., 2006. Parameters for the assessment of odour impacts on communities. Atmos. Environ. 40, 1016–1029.

LNE, 2008. Departement Leefmilieu, Natuur en Energie. Achtergronddocument Bij Het Visiedocument 'De Weg Naar Een Duurzaam Geurbeleid', p. 108.

Oettl, D., Ferrero, E., 2017. A simple model to assess odour hours for regulatory purposes. Atmos. Environ. 155, 162–173.

Oettl, D., Kropsch, M., Mandl, M., 2018. Odour assessment in the vicinity of a pig-fatting farm using field inspections (EN 16841-1) and dispersion modelling. Atmos. Environ. 181, 54–60.

Perry, S.G., Cimorelli, A.J., Painec, R.J., Brode, R.W., Weil, J.C., Venkatram, A., Wilson, R.B., Lee, R.F., Peters, W.D., 2005. AERMOD: A dispersion model for industrial source applications. Part II: Model performance against 17 field study databases. J. Appl. Meteorol. 44, 694–708.

Piringer, M., Knauder, W., Petz, E., Schauberger, G., 2015. A comparison of separation distances against odour annoyance calculated with two models. Atmos. Environ. 116, 22–35.

Piringer, M., Knauder, W., Petz, E., Schauberger, G., 2016. Factors influencing separation distances against odour annoyance calculated by Gaussian and Lagrangian dispersion models. Atmos. Environ. 140, 69–83.

Schauberger, G., Piringer, M., Petz, E., 2000. Diurnal and annual variation of the sensation distance of odour emitted by livestock buildings calculated by the Austrian odour dispersion model (AODM). Atmos. Environ. 34, 4839–4851.

Schauberger, G., Piringer, M., Petz, E., 2006. Odour episodes in the vicinity of livestock buildings: a qualitative comparison of odour complaint statistics with model calculations. Agric. Ecosyst. Environ. 114, 185–194.

Schauberger, G., Piringer, M., Schmitzer, R., Kamp, M., Sowa, A., Koch, R., Eckhof, W., Grimm, E., Kypke, J., Hartung, E., 2012. Concept to assess the human perception of odour by estimating short-time peak concentrations from one-hour mean values. Reply to a comment by Janicke et al. Atmos. Environ. 54, 624–628.

Schiffman, S.S., Williams, C.M., 2005. Science of odor as a potential health issue. J. Environ. Qual. 34, 129–138.

Shusterman, D., 1992. Critical review: the health significance of environmental odor pollution. Arch. Environ. Health 47, 76–87.

Sommer-Quabach, E., Piringer, M., Petz, E., Schauberger, G., 2014. Comparability of separation distances between odour sources and residential areas determined by various national odour impact criteria. Atmos. Environ. 95, 20–28.

Sucker, K., Both, R., Winneke, G., 2009. Review of adverse health effects of odours in field studies. Water Sci. Technol. 59 (7), 1281–1289.

TA-Luft, 2002. Technische Anleitung Zur Reinhaltung der Luft. First General Administrative Regulation Pertaining the Federal Immission Control Act. Federal Ministry for Environment, Nature Conservation and Nuclear Safety. English Version, p. 252.

Temel, O., van Beeck, J., 2017. Two-equation eddy viscosity models based on the Monin–Obukhov similarity theory. Appl. Math. Model. 42, 1–16.

U.S. EPA, 2000. Meteorological Monitoring Guidance for Regulatory Modeling Applications. EPA-454/R-99-005. North Caroline, Research Triangle Park.

U.S. EPA, 2008. AERSURFACE User's Guide. EPA-454/B-08-001 (Revised 01/16/2013). United States Environmental Protection Agency, Research Triangle Park, North Carolina.

U.S. EPA, 2016a. AERMOD Model Formulation and Evaluation. EPA-454/B-16-014. United States Environmental Protection Agency, Research Triangle Park, North Carolina.

U.S. EPA, 2016b. EPA-454/B-16-012. United States Environmental Protection Agency, Research Triangle Park, North Carolina User's Guide for the AERMOD Terrain Preprocessor (AERMAP).

U.S. EPA, 2016c. User's Guide for the AERMOD Meteorological Processor (AERMET). EPA-454/B-16-010. United States Environmental Protection Agency, Research Triangle Park, North Carolina.

U.S. EPA, 2017. Revisions to the Guideline on Air Quality Models: Enhancements to the AERMOD Dispersion Modeling System and Incorporation of Approaches to Address Ozone and Fine Particulate Matter. 40 CFR part 51, Appendix W. EPA–HQ–OAR–2015–0310; FRL–9956–23–OAR. United States Environmental Protection Agency Final rule.

VDI 3894 Part 1, 2011. Emissions and Immissions from Animal Husbandry - Housing Systems and Emissions - Pigs, Cattle, Poultry, Horses. Verein Deutscher Ingenieure, Berlin Beuth Verlag GmbH.

VDI 3894 Part 2, 2012. Emissions from and Impacts of Livestock Operations. Method to Determine Separation Distances. Odour. Verein Deutscher Ingenieure. Beuth Verlag GmbH, Berlin.

Willems, E., Monseré, T., Dierckx, J., 2015. Geactualiseerd richtlijnenboek milieueffectrapportage 'Basisrichtlijnen per activiteitengroep – Landbouwdieren'. Gent: ABO NV, juni 2011 – aangepast maart 2015, 146.

Please cite this article as: Brancher, M., et al., Assessing the inter-annual variability of separation distances around odour sources to protect the residents from odour annoyance, J. Environ. Sci. (2018), https://doi.org/10.1016/j.jes.2018.09.018